EFFECT OF THE SEPARATION WALL IN THE MIXING PROPERTIES OF COAXIAL JETS

***A. Talamelli*[1], *R. Örlü*[2] *and A. Segalini*[2]**

[1] ***Department of Industrial Engineering, University of Bologna, I-47100 Forlí, Italy***
[2] ***Linné FLOW Centre, KTH Mechanics, SE-100 44 Stockholm, Sweden***

alessandro.talamelli@unibo.it

Abstract

The velocity and mixing field of two coaxial jet configurations has been experimentally characterized by means of hot- and cold-wire anemometry to investigate the effect of the initial conditions on the flow development, and to determine the leading processes in the "mixing transition" of the two streams. Amongst the possible operating conditions, four configurations with different inner and outer jet bulk velocity pairs (U_i, U_o) have been spatially characterized in terms of velocity and mixing field covering a region where $0.5 \leq r_u = U_o/U_i \leq 3$ with two different separation wall geometries, namely a sharp and a thick separating wall. For high velocity ratios the difference between the two geometries appears small and inside the experimental accuracy. On the other hand, for nearly unitary velocity ratio and with the thick wall configuration, the presence of a strong wake instability increases the interpenetration between the two streams enhancing the mixing process.

1 Introduction

Two coaxial jets which interact and mix belong to the class of flows that are of great interest from both the research and industrial point of view. Even though they have a relatively simple geometry, the flow-field depends on many different parameters which, if they can be easily changed, make coaxial jets suitable for studies of different phenomena related to stability, mixing and turbulence. The definition of the variables able to effectively control the flow dynamics has high applicative potential because coaxial jets can be considered a prototype of many industrial burners, but still simple enough to be experimentally characterized in the laboratory.

Early investigations, see for instance Ko and Kwan (1976) and Dahm et al (1992), have focussed on the effects of the velocity ratio between outer and inner jet bulk velocity, $r_u = U_o/U_i$, on the flow field initial evolution pointing out that for $r_u \gg 1$ the outer jet shear layer instability is strong enough to drive the inner shear layer. This was confirmed by the experimental study of Rehab et al (1997) and the numerical simulations of da Silva et al (2003). They demonstrate that in this regime there is a clear dominance of the outer shear layer, which dictates the vortex formation frequency in both shear layers. This so called lock-in phenomenon, seems to hold until the velocity ratio is up to a critical value of around 8, after which there is a strong recirculating region in place of the inner jet potential core.

Conversely, inside a given range of velocity ratios close to 1, Buresti et al (1994) demonstrated that, for a thick enough separating wall, a new instability mechanism dominates the near field dynamics and vortices periodically shed behind the separation wall. This mechanism (already observed in turbofan engines as a strong noise source; Olsen and Karchmer, 1976) is passive and it does not require any external energy, making this phenomenon interesting from the control point of view.

A clear and exhaustive analysis of the mixing in a coaxial jet through the different phases of the mixing process, starting from the instability of the flow up to the onset of molecular mixing has been performed by Villermaux and Rehab (2000). In their work they stressed the importance of the presence of persistent large-scale structures, which, as a results of a primary instability of the flow, increases the interpenetration between the flows accelerating the mixing transition.

By means of inviscid linear spatial stability analysis on several coaxial jet base-flows, Talamelli and Gavarini (2006) provided a theoretical background by which the instability modes present in their geometry, and the range of operating parameters where a region of absolute instability was present, could be obtained. They found that two unstable modes were associated with the presence of the wake behind the inner duct wall. For sufficiently high velocity defects, and for a limited range of velocity ratios around unity, one of these last two modes may become locally absolutely unstable. In the same work the absolute instability frequency was theoretically estimated.

The shedding frequency has been recently thoroughly characterized by Segalini and Talamelli (2011) as function of the operating conditions. The results pointed out the existence of three regions with different dominant physical mechanisms: for $r_u \ll 1$ a clear dominance of the inner shear layer was observed, in agreement with the observations of Ko and Kwan (1976). On the other hand, for $r_u \gg 1$ the outer shear layer was instead driving the dynamics, as observed by da Silva et al (2003), while for $r_u \approx 1$ the vortex shedding was strong enough to dominate the dynamics. Buresti et al (1994) proposed that the shedding frequency should be determined by the thickness of the separating wall and by the average bulk velocity. Segalini and Talamelli (2011) improved this estimation by accounting for the thickness of the side boundary layers and for the velocity ratio.

As stated by Talamelli and Gavarini (2006), and underlined by Örlü et al (2008), only a thick enough wall can create the conditions for a significant wake instability. A threshold thickness value to the onset of the wake instability could be expressed by using the results of Dziomba and Fiedler (1985) where the authors, studying the effect of initial conditions on mixing layers, found that for a separating wall thickness of less than 50% of the sum of the displacement thickness of both boundary layers no effect in the self-similar region was noticeable.

Even though the instability process behind the wall has been studied theoretically and experimentally, the effect of the shedding phenomenon in the subsequent flow evolution is still unclear. It is clear that the flow field is strongly influenced in the near exit region, while the differences tend to disappear moving downstream, at least in a statistical sense. Here we would like to characterize experimentally both the velocity and mixing field limiting the analysis to the near exit region of a coaxial jet configuration. In particular, two different separating wall geometries have been tested in this paper to investigate the effect of different initial boundary conditions on the flow field in terms of geometrical boundaries, and fluid parameters as well, on the velocity and mixing characteristics. Even though the description of the effective mixing characteristics of the jet is quite complex (see Villermaux and Rehab, 2000), we believe that the presence of large scale structures may strongly influence the initial interpenetration between the two streams and therefore deeply affect the evolution of the mixture.

2 Experimental apparatus and measurement techniques

The experiments have been carried out in the *Coaxial Air Tunnel* (CAT) facility in the laboratory of the *Second Faculty of Engineering* in Forlí. A description of the facility can be found in Segalini and Talamelli (2011). In the present experiment, two types of separation walls between the two streams have been used. The first one has a thickness of $t/D_i = 0.1$, where D_i =50 mm is the inner jet diameter, and ends abruptly in a rectangular geometry. The second one ends with a sharp trailing edge, making the wake thickness negligible ($t/D_i \approx 0$) with respect to the sum of the side boundary layers thicknesses. In the following the aforementioned separating walls will be referred to as *thick* and *sharp*, respectively.

To characterize the mixing field the outer jet has been heated by means of electrical resistors placed at the inlets of the outer settling chamber. The amount of temperature increase has been kept small enough to consider the temperature as a passive scalar, while it has still been large enough to ensure a high temperature resolution.

The velocity measurements have been performed by means of a *DANTEC* 55P61 X-wire probe in combination with a home-made cold-wire probe with an 2.5 μm Platinum wire with a length-to-diameter ratio of 200. The cold-wire has been placed 0.5 mm upstream and apart from the X-wire with an angle of 35° to the X-wire, to reduce the blockage downstream the X-wire. The hot-wires have been operated in constant temperature (CT) mode with a resistance overheat ratio of 80%, whereas the cold-wire in constant current (CC) mode at a constant current of 0.5 mA, by means of an *DANTEC StreamLine* and an *AA-lab AN-1003* hot-wire anemometry system, respectively.

The cold- and hot-wires have been calibrated slightly upstream the inner nozzle against a thermocouple and Prandtl-tube, respectively. The axial and radial velocity as well as the temperature are acquired simultaneously and enable therefore the instantaneous compensation of the velocity readings as well as the calculation of the instantaneous heat fluxes.

In the following all capital letters will indicate mean quantities while primes will indicate standard deviations. Due to the axial symmetry of this geometry, a cylindrical coordinate system (x, r, ϕ) has been adopted with corresponding velocity vector components (u, v, w) to indicate the streamwise, radial and azimuthal velocity, respectively. In accordance with conventional notation, the temperature will be reported in dimensionless form

$$\theta\,(t) = \frac{T\,(t) - T_{amb}}{T_{max} - T_{amb}}\,, \qquad (1)$$

where $T\,(t)$ is the instantaneous temperature measured by the cold-wire, T_{max} and T_{amb} are the maximum exit and ambient temperature, respectively. The advantage of the above non-dimensionalization is that $\theta\,(t)$, being a passive scalar, will remain bounded between 0 and 1.

3 Results and discussion

Initial conditions

In order to analyze the stability properties of the flow that affect the mixing between the two streams, the details of the different boundary layers at the jets exit have to be fully documented. Details of the two inner boundary layers have been reported in table 1, where a set of power law coefficients are given to calculate the momentum thickness and the maximum rms amplitude for a given Reynolds number

Thick wall case BL properties								
	state	A	n	B	k	Λ	$\bar{H}$	δ_{99}/θ
BL1	laminar	0.4023	-0.4142	$3.565 \cdot 10^{-6}$	0.8425	3.126	2.393	7.046
BL2	laminar	0.354	-0.4208	$8.357 \cdot 10^{-5}$	0.5941	12.007	2.247	7.828

Sharp wall case BL properties								
	state	A	n	B	k	Λ	$\bar{H}$	δ_{99}/θ
BL1	turbulent	$4 \cdot 10^{-3}$	0.2785	7.036	-0.3745	N.D.	1.689	8.010
BL2	laminar	0.2187	-0.3387	$2.7 \cdot 10^{-3}$	0.1983	1.951	2.540	8.450

Table 1: Boundary layer properties for both separating wall geometries: Coefficients for the relations $\theta/D = A \cdot \mathrm{Re}^n$ and $u'_{max}/U_\infty = B \cdot \mathrm{Re}^k$, the Pohlhausen Λ coefficient, the mean shape factor $\bar{H}$ and the ratio δ_{99}/θ.

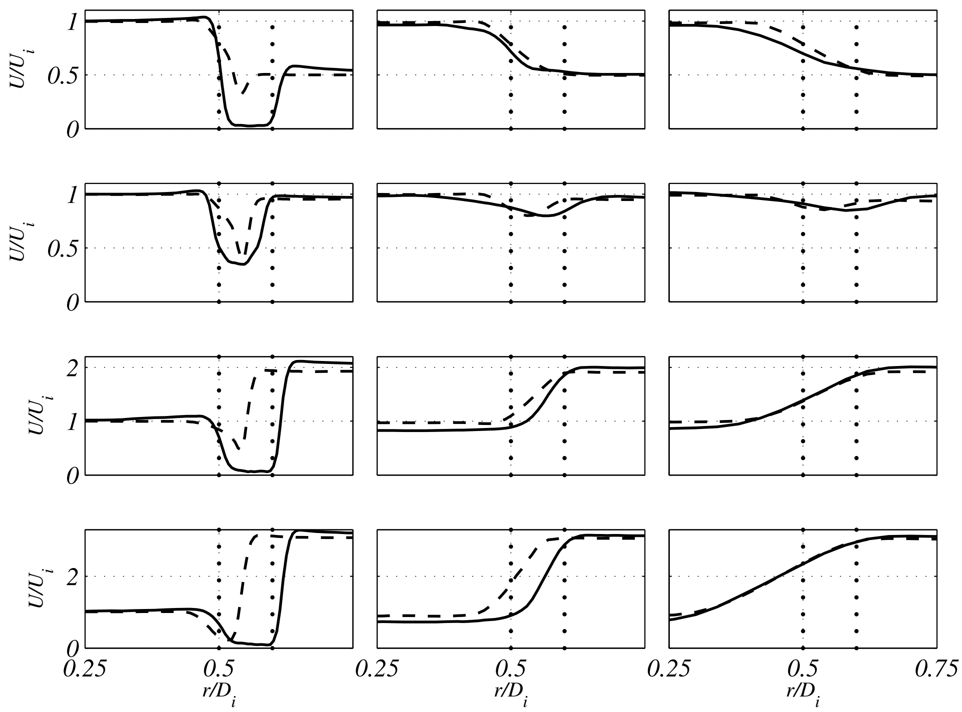

Figure 1: Radial profiles of the mean velocity for different velocity ratios (1$^{\mathrm{st}}$ *row*) $r_u \approx 0.5$, $\mathrm{Re} \approx 7000$; (2$^{\mathrm{nd}}$ *row*) $r_u \approx 1$, $\mathrm{Re} \approx 7000$; (3$^{\mathrm{rd}}$ *row*) $r_u \approx 2$, $\mathrm{Re} \approx 3500$; (4$^{\mathrm{th}}$ *row*) $r_u \approx 3$, $\mathrm{Re} \approx 1750$ at three streamwise stations (1$^{\mathrm{st}}$ *column*) $x/D_i = 0.04$, (2$^{\mathrm{nd}}$ *column*) $x/D_i = 1$, (3$^{\mathrm{rd}}$ *column*) $x/D_i = 2$ and different separating wall (*Solid line*) thick wall, (*Dashed line*) sharp wall. The dots indicate the radial locations of the thick wall.

$\mathrm{Re} = U_\infty D_i/\nu$ (U_∞ is the inner jet velocity for BL1 and outer jet velocity for BL2; cf. Segalini and Talamelli (2011) for definitions). Also, the average shape factor $\overline{H}$, δ_{99}/θ thickness ratio and the Pohlhausen Λ coefficient are reported to enable reconstruction of the boundary layers as an approximate polynomial function (Schlichting, 1968), in order to give a complete description of the initial conditions for future CFD comparisons.

It must be pointed out that while in the thick wall case, BL1 is still laminar and almost self-similar even at the lowest Reynolds number, this is not the case for the sharp separating wall where, due to the fact that the sharp wall presents a diverging section where the velocity decreases, the boundary layer BL1 appears to be still transitional and reaches the self-similar turbulent state for $Re_\theta \geq 500$. On the other hand, the boundary layer BL2 is laminar independently from the separating wall geometry as indicated in table 1.

Velocity field

It is well known that the velocity field plays a great role in the mixing process of a passive scalar. Therefore, a good characterization of the velocity field must be provided to understand the mixing process. Figure 1 reports the mean streamwise velocity profiles U/U_i for both geometries with the four velocity ratios considered here, as a subset of the available database. The first noticeable difference between the two geometries is due to the presence of a large wake component in the velocity profiles measured with the thick separating wall mounted. There is a slight overshoot in the velocity profiles close to the nozzle, probably accentuated by the thick trailing edge that generates a clear separating region and, consequently, a local accelera-

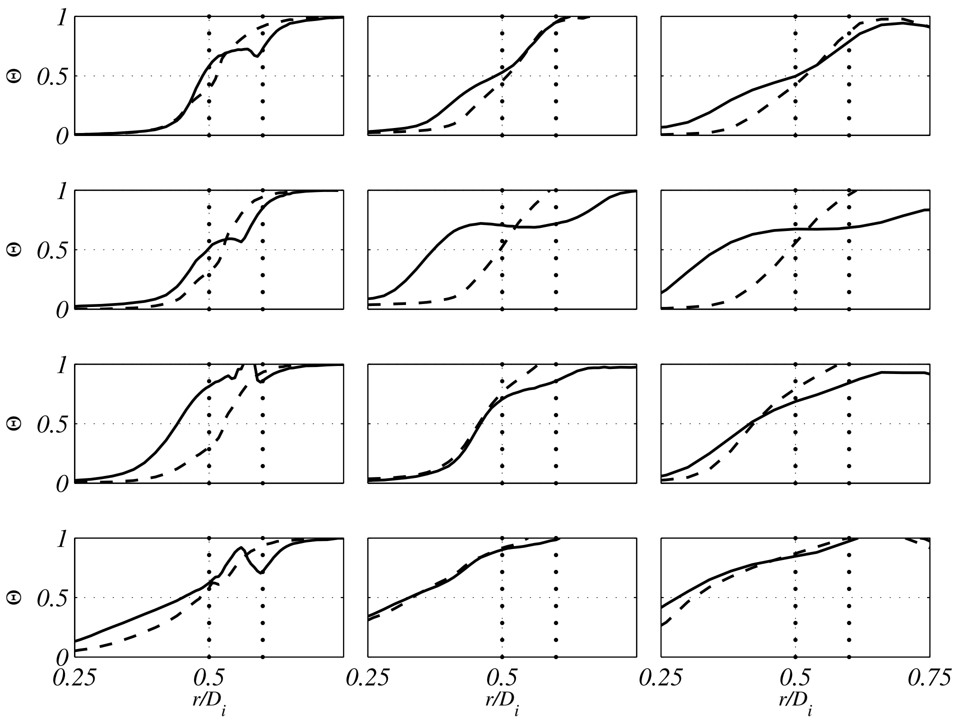

Figure 2: Radial profiles of the mean passive scalar concentration. See figure 1 for the caption.

tion of the flow close to the side boundary layers. This phenomenon is almost absent in the sharp wall case.

In the shear layer, the complex interactions of wake-mixing layers lead to a competition between the wake-like and the mixing layer-like behavior. The velocity defect in the U/U_i profile is a parameter that discerns whether or not the wake is still present. All investigated velocity ratios show wake traces immediately at the exit, but vanish after some distance from the nozzle due to transport mechanisms. The length of the region where the wake is observable is clearly a function of initial conditions and finds its maximum for a unitary velocity ratio and a thick wall geometry. Beside the unitary velocity ratio case, the wake seems to disappear downstream the first inner diameter, replaced by a shear layer, independently of the geometry of the separation wall.

Passive scalar profiles

The mean passive scalar evolution at different downstream stations is reported in figure 2. Although the initial passive scalar profile is not close to a top hat distribution, due to heat conduction across the settling chamber of both jets and the thermal inertia of the facility, the conclusions regarding the mixing evolution will be only partially affected by this and, nonetheless, the comparison between the different separating wall geometries can still be performed. Figure 2 shows that an increased mixing is evident only behind the thick wall configuration and for nearly unitary velocity ratios. At all other velocity ratios the difference between the two geometries appears small and within the experimental accuracy, clearly underlining that the presence of an absolute instability behind the wall is a key feature for the mixing behavior.

x/D	r_u	$thick$	$sharp$
0.5	0.5	0.126	0.101
0.5	1.0	0.205	0.091
0.5	2.0	0.131	0.112
0.5	3.0	0.333	0.254
1.5	0.5	0.183	0.121
1.5	1.0	0.330	0.082
1.5	2.0	0.206	0.145
1.5	3.0	0.245	0.243

Table 2: Mixing layer thickness, Δ, for different velocity ratios and streamwise positions according to (2).

The passive scalar distribution behind the wall allows the definition of a mixing thickness, Δ, as

$$\Delta = \frac{4}{\log 2}\int_0^{\eta} \Theta dr \quad \text{with} \quad \eta = r_x - \int_0^{r_x} \Theta dr \,, \tag{2}$$

where $r_x = 0.8D_i$ is the radial position where the centerline of the annular jet is located. The factor $4/\log 2$ is included so that the hyperbolic tangent profile

$$\Theta = \frac{1}{2}\left[1 + \tanh\left(\frac{r - r_0}{\delta}\right)\right] \qquad r_0 \gg 0 \,, \tag{3}$$

will have $\Delta = 2\delta$. The clear advantage of the proposed thickness is that it does not rely on the local derivative of the passive scalar profile (that can be significantly affected by measurement uncertainties), but

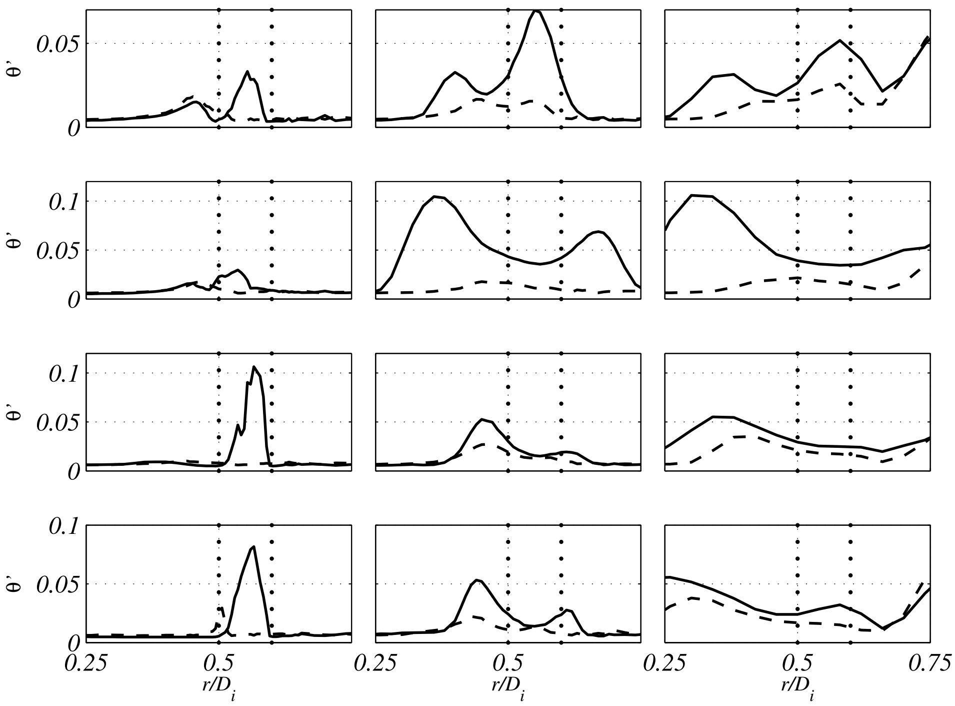

Figure 3: Radial profiles of the passive scalar standard deviation. See figure 1 for the caption.

rather on the integration of a part of the profile. Table 2 shows that a significant mixing enhancement is possible only at an almost unitary velocity ratio, and the differences reduce with the increase of the velocity ratio.

The radial profiles of the passive scalar standard deviation are reported in figure 3 furthermore underlining some aspects mentioned from the velocity field analysis, namely that the fluctuation level is a strong function of the velocity ratio, r_u, and of the initial conditions. In the shear layer region, in particular, the fluctuations are always enhanced when the thick separating wall is employed. This is also the case immediately at the jet exit and in the near field region (opposite to the velocity field), while the differences due to initial conditions decrease moving downstream for velocity ratios that depart from the unitary value. The $r_u = 1$ case exhibits a higher θ' with the thick wall even at $x/D_i = 4$ (not shown). A conjecture which explains this high level of fluctuation is that strong vortices are shed from the separating wall, each one containing a large amount of hot/cold unmixed fluid.

Figure 4 shows velocity and concentration power spectrum behind both thick and sharp separating wall. The figure, describing the energy content of the fluctuations at different frequencies, sheds some light in their nature and behavior. Behind the thick wall case the power spectrum of the concentration fluctuations indicates the passage of clear periodic disturbances with a peak located at frequencies, which correspond clearly to the primary instability of the wake (with their harmonics). Even though the sharp wall case does not produce any clear and distinct peak for the velocity field, the concentration fluctuations show some periodic activity even though with a low energy content, which is most probably related to the shear layer instability mode. Moving downstream (not shown in the picture) the spectra peaks become more and more reduced and they progressively lose the memory of the initial instability.

A confirmation of the presence of large scale patches of interpenetrated fluids, generated by means of a primary instability of the wake, can be assessed by extracting the coherent patches of hot and cold fluid through a conditional sampling technique. The trig-

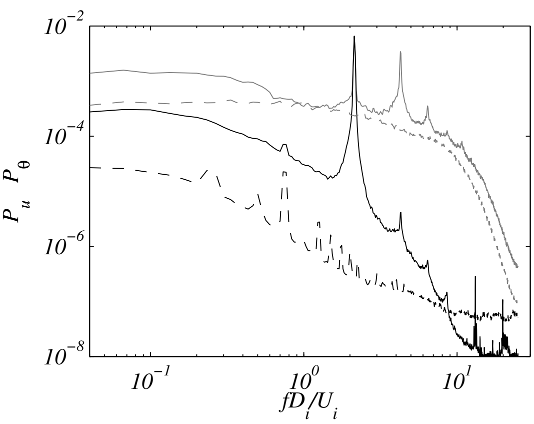

Figure 4: Velocity and concentration power spectral density at $r_u = 1$ for the thick (Solid lines) and sharp (Dashed lines) wall configuration at $x/D_i = 0.25$. The spectra are made dimensionless with the inner jet bulk velocity, U_i, and inner diameter, D_i. (Gray lines) P_u, (Black line) P_θ.

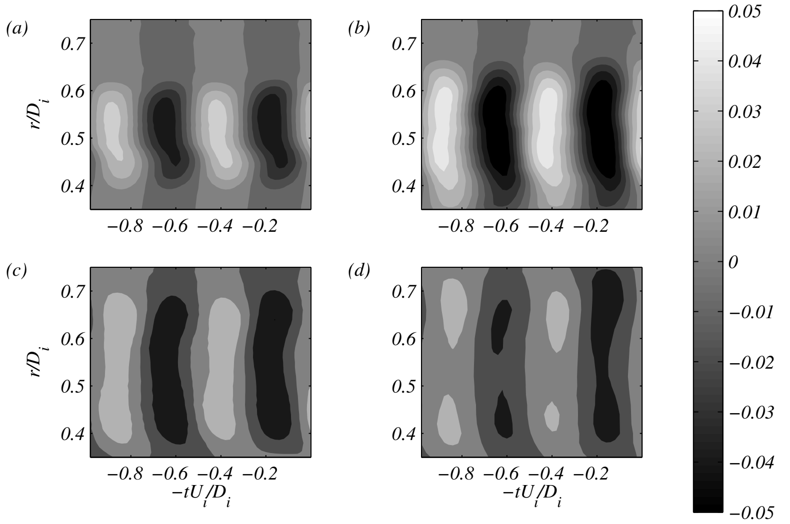

Figure 5: Conditionally educed scalar fluctuations at $r_u = 1$ for the thick wall configuration at (a) $x/D_i = 0.25$, (b) $x/D_i = 0.5$, (c) $x/D_i = 1$, (d) $x/D_i = 1.5$.

gering event has been defined as the time where the instantaneous radial velocity component exceeds its average by a certain percentage of its rms value (i.e. $v > V + \alpha v'$).

Figures 5 reports the conditionally sampled radial concentration fields with the thick wall for $r_u = 1$. The figure shows clearly the presence of interpenetrated patches which are originated from the wake instability. Moving downstream these still unmixed portions of fluid start to be stretched and deformed, becoming more and more mixed.

The other velocity ratios and the sharp wall related images are not presented because they are much more affected by the jittering effect and the structures are not clearly detectable with the adopted eduction method.

4 Conclusions

The effect of the nozzle geometry on the initial evolution of the velocity and mixing field of two coaxial jets has been discussed in terms of the operating parameters, namely the velocity ratio, $r_u = U_o/U_i$, and the geometry of the separation wall between the two streams.

The analysis of both the velocity and passive scalar concentration field has shown that the thick wall geometry, for velocity ratios close to one, is a key feature for a faster mixing process since it enhances the interpenetration of the two different streams. This is due to the presence of a clear vortex shedding phenomenon behind the thick separating wall which dominates the flow dynamics in the near field. This effect decreases significantly for small and large velocity ratios for which the shedding phenomenon disappears.

This behavior has also been quantified by means of a new thickness measure based on the mean scalar concentration.

Acknowledgments

Prof. Guido Buresti and Prof. Henrik Alfredsson are gratefully acknowledged. AT wishes to thank Italian MIUR for the financial support.

References

Buresti, G., Talamelli, A. and Petagna, P. (1994), Experimental characterization of the velocity field of a coaxial jet configuration *Exp. Therm. Fluid Sci.*, Vol. 9, pp. 135-146.

Dahm, W.J.A., Frieler, C.E. and Tryggvason, G. (1992), Vortex structure and dynamics in the near field of a coaxial jet, *J. Fluid Mech.*, Vol. 241, pp. 371-402.

Dziomba, B. and Fiedler, H. (1985), Effect of initial conditions on two-dimensional free shear layers *J. Fluid Mech.*, Vol. 152, pp. 419-442.

da Silva, C., Balarac, G. and Metais, O. (2003), Transition in high velocity ratio coaxial jets analysed from direct numerical simulations *J. Turbulence*, Vol. 24.

Ko, N.W.M. and Kwan, A.S.H. (1976), The initial region of subsonic coaxial jets, *J. Fluid Mech.*, Vol. 73, pp. 305-332

Olsen, W. and Karchmer, A. (1976), Lip noise generated by flow separation from nozzle surfaces, AIAA Paper 76-3.

Rehab, H., Villermaux, E. and Hopfinger, E. (1997),Flow regimes of large-velocity-ratio coaxial jets, *J. Fluid Mech.*, Vol. 345, pp. 357-381.

Schlichting, H. (1968) Boundary layer theory, 7th edn. McGraw-Hill.

Segalini, A. and Talamelli, A. (2011) Experimental analysis of dominant instabilities in coaxial jets, *Phys. Fluids*, Vol. 23-024103.

Talamelli, A. and Gavarini, I. (2006), Linear instability characteristics of incompressible coaxial jets, *Flow Turbul. Combust.*, Vol. 76-221-240.

Villermaux, E. and Rehab, H. (2000), Mixing in coaxial jets, *J. Fluid Mech.*, Vol. 425, pp. 161-185.

Örlü, R., Segalini, A. , Alfredsson, P.H. and Talamelli, A. (2008), On the passive control of the near-field of coaxial jets by means of vortex shedding, Proc. Int. Conf. Jets, Wakes and Separated Flows, ICJWSF-2008, TU Berlin, Germany, Sept. 1619, 2008.